Interaction curves for vibration and buckling of thin-walled composite box beams under axial loads and end moments

Thuc Phuong Vo* and Jaehong Lee†

Department of Architectural Engineering, Sejong University
98 Kunja Dong, Kwangjin Ku, Seoul 143-747, Korea

(Dated: January 14, 2010)

Interaction curves for vibration and buckling of thin-walled composite box beams with arbitrary lay-ups under constant axial loads and equal end moments are presented. This model is based on the classical lamination theory, and accounts for all the structural coupling coming from material anisotropy. The governing differential equations are derived from the Hamilton's principle. The resulting coupling is referred to as triply flexural-torsional coupled vibration and buckling. A displacement-based one-dimensional finite element model with seven degrees of freedoms per node is developed to solve the problem. Numerical results are obtained for thin-walled composite box beams to investigate the effects of axial force, bending moment, fiber orientation on the buckling loads, buckling moments, natural frequencies and corresponding vibration mode shapes as well as axial-moment-frequency interaction curves.

Keywords: Thin-walled composite box beams; classical lamination theory; axial loads and end moments; axial-moment-frequency interaction curves.

1. INTRODUCTION

Fiber-reinforced composite materials have been used over the past few decades in a variety of structures. Composites have many desirable characteristics, such as high ratio of stiffness and strength to weight, corrosion resistance and magnetic transparency. Thin-walled structural shapes made up of composite materials, which are usually produced by pultrusion, are being increasingly used in many civil, mechanical and aerospace engineering applications. How-

*Postdoctoral research fellow

†Professor, corresponding author. Tel.:+82-2-3408-3287; fax:+82-2-3408-3331

; Electronic address: jhlee@sejong.ac.kr

ever, it is well known that thin-walled composite structures might be under axial force and moment simultaneously when used in above applications and are very susceptible to flexural-torsional/lateral buckling and display complex vibrational behavior. Therefore, the accurate prediction of their stability limit state and dynamic characteristics is of the fundamental importance in the design of composite structures.

The theory of thin-walled members made of isotropic materials was first developed by Vlasov [1] and Gjelsvik [2]. Vibration and buckling of these members under axial loads and end moments becomes quite difficult problems when other than simple boundary conditions exist, where the cross-section has one or no axis of symmetry. Since the early works of Bleich et al. [3] and Timoshenko et al. [4,5], intensive research works have been conducted to develop theoretical beam models and analytical solutions for the stability and vibrational behavior of thin-walled beams. Joshi and Suryanarayan [6,7] derived closed form analytical solutions for flexural-torsional coupled instability and vibration of thin-walled beams under the combined action of axial loads and equal end moments. Pavlovic et al. [8] obtained closed form analytical solutions for dynamic stability problem of simply supported thin-walled beams under time-dependent stochastic axial loads and end moments. Based on a non-linear stability model, Mohri et al [9] proposed analytical solutions for simply supported beam-column elements with bi-symmetric I-sections under combined bending and axial forces. Magnucka-Blandzi [10] derived the general algebraic equation of the critical state for simply supported thin-walled beam under combined loads. Another effective approach for solving stability and dynamic problems of thin-walled beams is to develop the dynamic stiffness matrix based on the solution of simultaneous ordinary differential equations. By using the power series method, Leung [11,12] derived the exact dynamic stiffness matrix including both the axial force, initial torque and bending moment for the interactive axial-torsional and axial-moment buckling analysis of framed structures. Besides, the finite element method has been widely used because of its versatility and much efforts have been devoted in order to obtain accurate results. Mohri et al. [13] presented a higher-order non shear deformable model to investigate the dynamic behavior of thin-walled open sections in the pre- and post-buckling state. Bebiano et al. [14] illustrated the application of a novel Generalised Beam Theory (GBT) formulation to analyze the local-plate, distortional and global vibration behavior of thin-walled steel channel members subjected to compression and/or non-uniform bending. Voros [15] analyzed the free vibration and mode shapes of straight beams where the coupling between the bending and torsion was induced by steady state lateral loads. For thin-walled composite beams, with the presence of the additional coupling effects from material anisotropy, these members under axial force and moment simultaneously exhibit strong coupling. Thus, their dynamic characteristics become more complicated than isotropic material even for doubly symmetric cross-section. Even though a significant

amount of research has been conducted on the dynamic characteristics of axially loaded thin-walled open and closed section composite beams (Bank and Kao [16], Banerjee et al. [17,18], Li et al. [19,20], Kaya and Ozgumus [21] and Kim and Shin [22]), it should be noted that only a few have taken into account the effects of axial force and bending moment. Machado et al. [23] investigated the influence of the initial in-plane deformations, generated by the action of a static external loading, as well as the effect of shear flexibility on the dynamic behavior of bisymmetric thin-walled composite beams. The analysis was based on a geometrically non-linear theory based on large displacements and rotations. However, it was strictly valid for symmetric balanced laminates and especially orthotropic laminates. A literature survey on the subject has revealed that studies of vibration and buckling of thin-walled composite box beams with arbitrary lay-ups including the influences of axial force and bending moment in a unitary manner are limited. To the best of the authors' knowledge, there is no publication available that deals with axial-moment-frequency interaction curves for vibration and buckling of thin-walled composite box beams in the open literature. This complicated problem is not well-investigated and there is a need for further studies.

In this paper, which is an extension of the authors' previous works [24-26], flexural-torsional coupled vibration and buckling of thin-walled composite box beams with arbitrary lay-ups under constant axial loads and equal end moments is presented. This model is based on the classical lamination theory, and accounts for all the structural coupling coming from the material anisotropy. The governing differential equations for flexural-torsional coupled vibration are derived from the Hamilton's principle. A displacement-based one-dimensional finite element model with seven degrees of freedoms per node is developed to solve the problem. Numerical results are obtained for thin-walled composite box beams to investigate the effects of axial force, bending moment, fiber orientation on the buckling loads, buckling moments, natural frequencies and corresponding vibration mode shapes as well as axial-moment-frequency interaction curves.

2. KINEMATICS

The theoretical developments presented in this paper require two sets of coordinate systems which are mutually interrelated. The first coordinate system is the orthogonal Cartesian coordinate system (x, y, z), for which the x and y axes lie in the plane of the cross section and the z axis parallel to the longitudinal axis of the beam. The second coordinate system is the local plate coordinate (n, s, z) as shown in Fig. 1, wherein the n axis is normal to the middle surface of a plate element, the s axis is tangent to the middle surface and is directed along the contour line of the cross section. The (n, s, z) and (x, y, z) coordinate systems are related through an angle of orientation θ. As defined

in Fig.1 a point P, called the pole, is placed at an arbitrary point x_p, y_p. A line through P parallel to the z axis is called the pole axis.

To derive the analytical model for a thin-walled composite beam, the following assumptions are made:

1. The contour of the thin wall does not deform in its own plane.
2. The linear shear strain $\bar{\gamma}_{sz}$ of the middle surface has the same distribution in the contour direction as it does in the St. Venant torsion in each element.
3. The Kirchhoff-Love assumption in classical plate theory remains valid for laminated composite thin-walled beams.
4. Each laminate is thin and perfectly bonded.
5. Local buckling is not considered.

According to assumption 1, the midsurface displacement components $\bar{u}, \bar{v}$ at a point A in the contour coordinate system can be expressed in terms of a displacements U, V of the pole P in the x, y directions, respectively, and the rotation angle Φ about the pole axis,

$$\bar{u}(s,z) = U(z)\sin\theta(s) - V(z)\cos\theta(s) - \Phi(z)q(s) \tag{1a}$$

$$\bar{v}(s,z) = U(z)\cos\theta(s) + V(z)\sin\theta(s) + \Phi(z)r(s) \tag{1b}$$

These equations apply to the whole contour. The out-of-plane shell displacement $\bar{w}$ can now be found from the assumption 2. For each element of middle surface, the shear strain become

$$\bar{\gamma}_{sz} = \frac{\partial \bar{v}}{\partial z} + \frac{\partial \bar{w}}{\partial s} = \Phi'(z)\frac{F(s)}{t(s)} \tag{2}$$

where $t(s)$ is thickness of contour box section, $F(s)$ is the St. Venant circuit shear flow. After substituting for $\bar{v}$ from Eq.(1) and considering the following geometric relations,

$$dx = ds\cos\theta \tag{3a}$$

$$dy = ds\sin\theta \tag{3b}$$

Eq.(2) can be integrated with respect to s from the origin to an arbitrary point on the contour,

$$\bar{w}(s,z) = W(z) - U'(z)x(s) - V'(z)y(s) - \Phi'(z)\omega(s) \tag{4}$$

where differentiation with respect to the axial coordinate z is denoted by primes ($'$); W represents the average axial displacement of the beam in the z direction; x and y are the coordinates of the contour in the (x, y, z) coordinate system; and ω is the so-called sectorial coordinate or warping function given by

$$\omega(s) = \int_{s_\circ}^{s} \Big[r(s) - \frac{F(s)}{t(s)}\Big] ds \tag{5a}$$

$$\oint_i \frac{F(s)}{t(s)} ds = 2A_i \quad i = 1, ..., n \tag{5b}$$

where $r(s)$ is height of a triangle with the base ds; A_i is the area circumscribed by the contour of the i circuit. The explicit forms of $\omega(s)$ and $F(s)$ for box section are given in Ref.[25].

The displacement components u, v, w representing the deformation of any generic point on the profile section are given with respect to the midsurface displacements $\bar{u}, \bar{v}, \bar{w}$ by the assumption 3.

$$u(s, z, n) = \bar{u}(s, z) \tag{6a}$$

$$v(s, z, n) = \bar{v}(s, z) - n\frac{\partial \bar{u}(s, z)}{\partial s} \tag{6b}$$

$$w(s, z, n) = \bar{w}(s, z) - n\frac{\partial \bar{u}(s, z)}{\partial z} \tag{6c}$$

The strains associated with the small-displacement theory of elasticity are given by

$$\epsilon_s = \bar{\epsilon}_s + n\bar{\kappa}_s \tag{7a}$$

$$\epsilon_z = \bar{\epsilon}_z + n\bar{\kappa}_z \tag{7b}$$

$$\gamma_{sz} = \bar{\gamma}_{sz} + n\bar{\kappa}_{sz} \tag{7c}$$

where

$$\bar{\epsilon}_s = \frac{\partial \bar{v}}{\partial s}; \quad \bar{\epsilon}_z = \frac{\partial \bar{w}}{\partial z} \tag{8a}$$

$$\bar{\kappa}_s = -\frac{\partial^2 \bar{u}}{\partial z^2}; \quad \bar{\kappa}_z = -\frac{\partial^2 \bar{u}}{\partial z^2}; \quad \bar{\kappa}_{sz} = -2\frac{\partial^2 \bar{u}}{\partial s \partial z} \tag{8b}$$

All the other strains are identically zero. In Eq.(8), $\bar{\epsilon}_s$ and $\bar{\kappa}_s$ are assumed to be zero. $\bar{\epsilon}_z$, $\bar{\kappa}_z$ and $\bar{\kappa}_{sz}$ are midsurface axial strain and biaxial curvature of the shell, respectively. The above shell strains can be converted to beam strain components by substituting Eqs.(1), (4) and (6) into Eq.(8) as

$$\bar{\epsilon}_z = \epsilon_z^\circ + x\kappa_y + y\kappa_x + \omega\kappa_\omega \tag{9a}$$

$$\bar{\kappa}_z = \kappa_y \sin\theta - \kappa_x \cos\theta - \kappa_\omega q \tag{9b}$$

$$\bar{\kappa}_{sz} = 2\bar{\chi}_{sz} = \kappa_{sz} \tag{9c}$$

where $\epsilon_z^\circ, \kappa_x, \kappa_y, \kappa_\omega$ and κ_{sz} are axial strain, biaxial curvatures in the $x-$ and y-direction, warping curvature with respect to the shear center, and twisting curvature in the beam, respectively defined as

$$\epsilon_z^\circ = W' \tag{10a}$$

$$\kappa_x = -V'' \tag{10b}$$

$$\kappa_y = -U'' \tag{10c}$$

$$\kappa_\omega = -\Phi'' \tag{10d}$$

$$\kappa_{sz} = 2\Phi' \tag{10e}$$

The resulting strains can be obtained from Eqs.(7) and (9) as

$$\epsilon_z = \epsilon_z^\circ + (x + n\sin\theta)\kappa_y + (y - n\cos\theta)\kappa_x + (\omega - nq)\kappa_\omega \tag{11a}$$

$$\gamma_{sz} = (n + \frac{F}{2t})\kappa_{sz} \tag{11b}$$

3. VARIATIONAL FORMULATION

The total potential energy of the system can be stated, in its buckled shape, as

$$\Pi = \mathcal{U} + \mathcal{V} \tag{12}$$

where $\mathcal{U}$ is the strain energy

$$\mathcal{U} = \frac{1}{2}\int_v (\sigma_z\epsilon_z + \sigma_{sz}\gamma_{sz})dv \tag{13}$$

After substituting Eq.(11) into Eq.(13)

$$\mathcal{U} = \frac{1}{2}\int_v \left\{\sigma_z\Big[\epsilon_z^\circ + (x + n\sin\theta)\kappa_y + (y - n\cos\theta)\kappa_x + (\omega - nq)\kappa_\omega\Big] + \sigma_{sz}n\kappa_{sz}\right\}dv \tag{14}$$

The variation of strain energy can be stated as

$$\delta\mathcal{U} = \int_0^l (N_z\delta\epsilon_z + M_y\delta\kappa_y + M_x\delta\kappa_x + M_\omega\delta\kappa_\omega + M_t\delta\kappa_{sz})dz \tag{15}$$

where $N_z, M_x, M_y, M_\omega, M_t$ are axial force, bending moments in the x- and y-direction, warping moment (bimoment), and torsional moment with respect to the centroid, respectively, defined by integrating over the cross-sectional area A

as

$$N_z = \int_A \sigma_z dsdn \tag{16a}$$

$$M_y = \int_A \sigma_z (x + n\sin\theta) dsdn \tag{16b}$$

$$M_x = \int_A \sigma_z (y - n\cos\theta) dsdn \tag{16c}$$

$$M_\omega = \int_A \sigma_z (\omega - nq) dsdn \tag{16d}$$

$$M_t = \int_A \sigma_{sz} n dsdn \tag{16e}$$

The potential of in-plane loads $\mathcal{V}$ due to transverse deflection

$$\mathcal{V} = \frac{1}{2}\int_v \overline{\sigma}_z^0 \Big[(u')^2 + (v')^2\Big] dv \tag{17}$$

where $\overline{\sigma}_z^0$ is the averaged constant in-plane edge axial stress of beams loaded initially by equal and opposite axial forces P and bending moment M_x^0 at two ends, defined by

$$\overline{\sigma}_z^0 = \frac{P_0}{A} - \frac{M_x^0 y}{I_x} \tag{18}$$

The variation of the potential of in-plane loads at the centroid is expressed by substituting the assumed displacement field into Eq.(17) as

$$\begin{aligned}\delta\mathcal{V} = \int_v (\frac{P_0}{A} - \frac{M_x^0 y}{I_x}) \Big[& U'\delta U' + V'\delta V' + (q^2 + r^2 + 2rn + n^2)\Phi'\delta\Phi' \\ & + (\Phi'\delta U' + U'\delta\Phi')\big[n\cos\theta - (y - y_p)\big] + (\Phi'\delta V' + V'\delta\Phi')\big[n\cos\theta + (x - x_p)\big]\Big] dv\end{aligned} \tag{19}$$

The kinetic energy of the system is given by

$$\mathcal{T} = \frac{1}{2}\int_v \rho(\dot{u}^2 + \dot{v}^2 + \dot{w}^2) dv \tag{20}$$

where ρ is a density.

The variation of the kinetic energy is expressed by substituting the assumed displacement field into Eq.(20) as

$$\begin{aligned}\delta\mathcal{T} = \int_v \rho\Big\{ & \dot{U}\delta\dot{U} + \dot{V}\delta\dot{V} + \dot{W}\delta\dot{W} + (q^2 + r^2 + 2rn + n^2)\dot{\Phi}\delta\dot{\Phi} + (\dot{\Phi}\delta\dot{U} + \dot{U}\delta\dot{\Phi})\Big[n\cos\theta - (y - y_p)\Big] \\ & + (\dot{\Phi}\delta\dot{V} + \dot{V}\delta\dot{\Phi})\Big[n\cos\theta + (x - x_p)\Big]\Big\} dv\end{aligned} \tag{21}$$

In order to derive the equations of motion, Hamilton's principle is used

$$\delta\int_{t_1}^{t_2} (\mathcal{T} - \Pi) dt = 0 \tag{22}$$

Substituting Eqs.(15), (19) and (21) into Eq.(22), the following weak statement is obtained

$$\begin{aligned} 0 \;=\; & \int_{t_1}^{t_2}\int_0^l \Big\{ m_0\dot{W}\delta\dot{W} + \Big[m_0\dot{U} + (m_c + m_0 y_p)\dot{\Phi}\Big]\delta\dot{U} + \Big[m_0\dot{V} + (m_s - m_0 x_p)\dot{\Phi}\Big]\delta\dot{V} \\ & + \Big[(m_c + m_0 y_p)\dot{U} + (m_s - m_0 x_p)\dot{V} + (m_p + m_2 + 2m_\omega)\dot{\Phi}\Big]\delta\dot{\Phi} \\ & - \Big[P_0\big[\delta U'(U' + \Phi' y_p) + \delta V'(V' - \Phi' x_p) + \delta\Phi'(\Phi'\frac{I_p}{A} + U' y_p - V' x_p)\big] - M_x^0(\Phi\delta U'' + U''\delta\Phi)\Big] \\ & - N_z\delta W' + M_y\delta U'' + M_x\delta V'' + M_\omega\delta\Phi'' - 2M_t\delta\Phi\Big\} dzdt \end{aligned} \tag{23}$$

The explicit expressions of inertia coefficients for thin-walled composite box beams are given in Ref.[26].

4. CONSTITUTIVE EQUATIONS

The constitutive equations of a k^{th} orthotropic lamina in the laminate co-ordinate system of section are given by

$$\begin{Bmatrix} \sigma_z \\ \sigma_{sz} \end{Bmatrix}^k = \begin{bmatrix} \bar{Q}_{11}^* & \bar{Q}_{16}^* \\ \bar{Q}_{16}^* & \bar{Q}_{66}^* \end{bmatrix}^k \begin{Bmatrix} \epsilon_z \\ \gamma_{sz} \end{Bmatrix} \tag{24}$$

where $\bar{Q}_{ij}^*$ are transformed reduced stiffnesses. The transformed reduced stiffnesses can be calculated from the transformed stiffnesses based on the plane stress ($\sigma_s = 0$) and plane strain ($\epsilon_s = 0$) assumption. More detailed explanation can be found in Ref.[27].

The constitutive equations for bar forces and bar strains are obtained by using Eqs.(11), (16) and (24)

$$\begin{Bmatrix} N_z \\ M_y \\ M_x \\ M_\omega \\ M_t \end{Bmatrix} = \begin{bmatrix} E_{11} & E_{12} & E_{13} & E_{14} & E_{15} \\ & E_{22} & E_{23} & E_{24} & E_{25} \\ & & E_{33} & E_{34} & E_{35} \\ & & & E_{44} & E_{45} \\ \text{sym.} & & & & E_{55} \end{bmatrix} \begin{Bmatrix} \epsilon_z^\circ \\ \kappa_y \\ \kappa_x \\ \kappa_\omega \\ \kappa_{sz} \end{Bmatrix} \tag{25}$$

where E_{ij} are the laminate stiffnesses of thin-walled composite beams and given in Ref.[25].

5. GOVERNING EQUATIONS OF MOTION

The governing equations of motion of the present study can be derived by integrating the derivatives of the varied quantities by parts and collecting the coefficients of of $\delta W, \delta U, \delta V$ and $\delta\Phi$

$$N_z' = m_0\ddot{W} \tag{26a}$$

$$M_y'' + P_0\big(U'' + \Phi'' y_p\big) + M_x^0\Phi'' = m_0\ddot{U} + (m_c + m_0 y_p)\ddot{\Phi} \tag{26b}$$

$$M_x'' + P_0\big(V'' - \Phi'' x_p\big) = m_0\ddot{V} + (m_s - m_0 x_p)\ddot{\Phi} \tag{26c}$$

$$\begin{aligned} M_\omega'' + 2M_t' + P_0\big(\Phi''\frac{I_p}{A} + U'' y_p - V'' x_p\big) + M_x^0 U'' &= (m_c + m_0 y_p)\ddot{U} \\ &+ (m_s - m_0 x_p)\ddot{V} \\ &+ (m_p + m_2 + 2m_\omega)\ddot{\Phi} \end{aligned} \tag{26d}$$

The natural boundary conditions are of the form

$$\delta W \ : \ N_z = P_0 \tag{27a}$$

$$\delta U \ : \ M_y' = {M_y'}^0 \tag{27b}$$

$$\delta U' \ : \ M_y = M_y^0 \tag{27c}$$

$$\delta V \ : \ M_x' = {M_x'}^0 \tag{27d}$$

$$\delta V' \ : \ M_x = M_x^0 \tag{27e}$$

$$\delta\Phi \ : \ M_\omega' + 2M_t = {M_\omega'}^0 \tag{27f}$$

$$\delta\Phi' \ : \ M_\omega = M_\omega^0 \tag{27g}$$

where $P_0, {M_y'}^0, M_y^0, {M_x'}^0, M_x^0, {M_\omega'}^0$ and M_ω^0 are prescribed values.

By substituting Eqs.(10) and (25) into Eq.(26), the explicit form of governing equations of motion can be expressed

with respect to the laminate stiffnesses E_{ij} as

$$E_{11}W'' - E_{12}U''' - E_{13}V''' - E_{14}\Phi''' + 2E_{15}\Phi'' = m_0\ddot{W} \tag{28a}$$

$$E_{12}W''' - E_{22}U^{iv} - E_{23}V^{iv} - E_{24}\Phi^{iv} + 2E_{25}\Phi''' + P_0(U'' + \Phi'' y_p) + M_x^0\Phi'' = m_0\ddot{U} + (m_c + m_0 y_p)\ddot{\Phi} \tag{28b}$$

$$E_{13}W''' - E_{23}U^{iv} - E_{33}V^{iv} - E_{34}\Phi^{iv} + 2E_{35}\Phi''' + P_0(V'' - \Phi'' x_p) = m_0\ddot{V} + (m_s - m_0 x_p)\ddot{\Phi} \tag{28c}$$

$$\begin{aligned} E_{14}W''' + 2E_{15}W'' - E_{24}U^{iv} - 2E_{25}U''' - E_{34}V^{iv} - 2E_{35}V''' \\ -E_{44}\Phi^{iv} + 4E_{55}\Phi'' + P_0(\Phi''\frac{I_p}{A} + U'' y_p - V'' x_p) + M_x^0 U'' &= (m_c + m_0 y_p)\ddot{U} \\ &+ (m_s - m_0 x_p)\ddot{V} \\ &+ (m_p + m_2 + 2m_\omega)\ddot{\Phi} \end{aligned} \tag{28d}$$

Eq.(28) is most general form for flexural-torsional coupled vibration of thin-walled composite beams with arbitrary lay-ups under constant axial loads and equal end moments and the dependent variables, W, U, V and Φ are fully coupled. If all the coupling effects and the cross section is symmetrical with respect to both x- and the y-axes, Eq.(28) can be simplified to the uncoupled differential equations as

$$(EA)_{com}W'' = \rho A\ddot{W} \tag{29a}$$

$$-(EI_y)_{com}U^{iv} + P_0U'' + M_x^0\Phi'' = \rho A\ddot{U} \tag{29b}$$

$$-(EI_x)_{com}V^{iv} + P_0V'' = \rho A\ddot{V} \tag{29c}$$

$$-(EI_\omega)_{com}\Phi^{iv} + \Big[(GJ)_{com} + P_0\frac{I_p}{A}\Big]\Phi'' + M_x^0U'' = \rho I_p\ddot{\Phi} \tag{29d}$$

From above equations, $(EA)_{com}$ represents axial rigidity, $(EI_x)_{com}$ and $(EI_y)_{com}$ represent flexural rigidities with respect to x- and y-axis, $(EI_\omega)_{com}$ represents warping rigidity, and $(GJ)_{com}$ represents torsional rigidity of thin-walled composite beams, respectively, written as

$$(EA)_{com} = E_{11} \tag{30a}$$

$$(EI_y)_{com} = E_{22} \tag{30b}$$

$$(EI_x)_{com} = E_{33} \tag{30c}$$

$$(EI_\omega)_{com} = E_{44} \tag{30d}$$

$$(GJ)_{com} = 4E_{55} \tag{30e}$$

A. Flexural-torsional buckling under axial loads and equal end moments

By omitting the inertia terms, Eq.(29) becomes

$$(EA)_{com}W'' = 0 \tag{31a}$$

$$-(EI_y)_{com}U^{iv} + P_0U'' + M_x^0\Phi'' = 0 \tag{31b}$$

$$-(EI_x)_{com}V^{iv} + P_0V'' = 0 \tag{31c}$$

$$-(EI_\omega)_{com}\Phi^{iv} + \Big[(GJ)_{com} + P_0\frac{I_p}{A}\Big]\Phi'' + M_x^0U''' = 0 \tag{31d}$$

It is well known that the flexural buckling loads in the x-direction are identified while the flexural buckling loads in the y-direction, torsional buckling loads and buckling moments are coupled. The orthotropy solution for the critical values of axial force P_0 and bending moment M_x^0 for simply supported boundary condition [4]

$$M_x^0 = r_p\sqrt{P_\theta P_y(1-\frac{P_0}{P_y})(1-\frac{P_0}{P_\theta})} \tag{32}$$

where P_x, P_y and P_θ are the critical flexural buckling load in the x- and y-direction, and the critical torsional buckling load [4].

$$P_x = \frac{\pi^2(EI_x)_{com}}{l^2} \tag{33a}$$

$$P_y = \frac{\pi^2(EI_y)_{com}}{l^2} \tag{33b}$$

$$P_\theta = \frac{A}{I_p}\Big[\frac{\pi^2(EI_\omega)_{com}}{l^2} + (GJ)_{com}\Big] \tag{33c}$$

B. Flexural-torsional vibration under axial loads and equal end moments

For simply supported beams with free warping, the overall displacements modes in bending and torsion are assumed as

$$U(z,t) = U_0\sin(\frac{n\pi z}{L})\sin(\omega t) \tag{34a}$$

$$V(z,t) = V_0\sin(\frac{n\pi z}{L})\sin(\omega t) \tag{34b}$$

$$\Phi(z,t) = \Phi_0\sin(\frac{n\pi z}{L})\sin(\omega t) \tag{34c}$$

Substituting Eq.(34) into Eq.(29), after integrations and some reductions, the resulting flexural and torsional equations of motion are obtained in compact form as

$$\omega_{x_n}^2(1-\overline{P}_{x_n}) - \omega_{xx_n}^2 = 0 \tag{35a}$$

$$A\Big[\omega_{y_n}^2(1-\overline{P}_{y_n}) - \omega^2\Big]U_0 - \overline{M}_{x_n}\sqrt{AI_p}\omega_{y_n}\omega_{\theta_n}\Phi_0 = 0 \tag{35b}$$

$$-\overline{M}_{x_n}\sqrt{AI_p}\omega_{y_n}\omega_{\theta_n}U_0 + I_p\Big[\omega_{\theta_n}^2(1-\overline{P}_{\theta_n}) - \omega^2\Big]\Phi_0 = 0 \tag{35c}$$

For the above equations, it is well known that the flexural natural frequencies in the x-direction and bending moments are decoupled, while, the flexural natural frequencies in the y-direction, torsional natural frequencies and bending moments are coupled. They are given by the orthotropy solution for simply supported boundary condition

$$\omega_{xx_n} = \omega_{x_n}\sqrt{1-\overline{P}_{x_n}} \tag{36a}$$

$$\omega_{ya_n} = \sqrt{\frac{\omega_{y_n}^2(1-\overline{P}_{y_n}) + \omega_{\theta_n}^2(1-\overline{P}_{\theta_n})}{2} - \sqrt{\Big[\frac{\omega_{y_n}^2(1-\overline{P}_{y_n}) - \omega_{\theta_n}^2(1-\overline{P}_{\theta_n})}{2}\Big]^2 + \overline{M}_n^2\omega_{y_n}^2\omega_{\theta_n}^2}} \tag{36b}$$

$$\omega_{yb_n} = \sqrt{\frac{\omega_{y_n}^2(1-\overline{P}_{y_n}) + \omega_{\theta_n}^2(1-\overline{P}_{\theta_n})}{2} + \sqrt{\Big[\frac{\omega_{y_n}^2(1-\overline{P}_{y_n}) - \omega_{\theta_n}^2(1-\overline{P}_{\theta_n})}{2}\Big]^2 + \overline{M}_n^2\omega_{y_n}^2\omega_{\theta_n}^2}} \tag{36c}$$

in which $\overline{P}_{x_n}, \overline{P}_{y_n}, \overline{P}_{\theta_n}$ and $\overline{M}_{x_n}$ are nondimensional axial force and moment parameters

$$\overline{P}_{x_n} = \frac{P_0}{P_{x_n}} \tag{37a}$$

$$\overline{P}_{y_n} = \frac{P_0}{P_{y_n}} \tag{37b}$$

$$\overline{P}_{\theta_n} = \frac{P_0}{P_{\theta_n}} \tag{37c}$$

$$\overline{M}_{x_n} = \frac{M_x^0}{M_{y\theta_n}} \tag{37d}$$

where P_{x_n}, P_{y_n} and P_{θ_n} are the flexural buckling loads in the x- and y-direction, and torsional buckling loads [4].

$$P_{x_n} = \frac{n^2\pi^2(EI_x)_{com}}{l^2} \tag{38a}$$

$$P_{y_n} = \frac{n^2\pi^2(EI_y)_{com}}{l^2} \tag{38b}$$

$$P_{\theta_n} = \frac{A}{I_p}\Big[\frac{n^2\pi^2(EI_\omega)_{com}}{l^2} + (GJ)_{com}\Big] \tag{38c}$$

and $M_{y\theta_n}$ is the buckling moments for pure bending [4].

$$M_{y\theta_n} = \sqrt{\frac{n^2\pi^2(EI_y)_{com}}{l^2}\Big[\frac{n^2\pi^2(EI_\omega)_{com}}{l^2} + (GJ)_{com}\Big]} \tag{39}$$

and $\omega_{x_n}, \omega_{y_n}$ and ω_{θ_n} are the flexural natural frequencies in the x- and y-direction, and torsional natural frequencies [5].

$$\omega_{x_n} = \frac{n^2\pi^2}{l^2}\sqrt{\frac{(EI_x)_{com}}{\rho A}} \tag{40a}$$

$$\omega_{y_n} = \frac{n^2\pi^2}{l^2}\sqrt{\frac{(EI_y)_{com}}{\rho A}} \tag{40b}$$

$$\omega_{\theta_n} = \frac{n\pi}{l}\sqrt{\frac{1}{\rho I_p}\Big[\frac{n^2\pi^2}{l^2}(EI_\omega)_{com} + (GJ)_{com}\Big]} \tag{40c}$$

6. FINITE ELEMENT FORMULATION

The present theory for thin-walled composite beams described in the previous section was implemented via a displacement based finite element method. The element has seven degrees of freedom at each node, three displacements W, U, V and three rotations U', V', Φ as well as one warping degree of freedom Φ'. The axial displacement W is interpolated using linear shape functions Ψ_j, whereas the lateral and vertical displacements U, V and axial rotation Φ are interpolated using Hermite-cubic shape functions ψ_j associated with node j and the nodal values, respectively.

$$W = \sum_{j=1}^{2} w_j \Psi_j \tag{41a}$$

$$U = \sum_{j=1}^{4} u_j \psi_j \tag{41b}$$

$$V = \sum_{j=1}^{4} v_j \psi_j \tag{41c}$$

$$\Phi = \sum_{j=1}^{4} \phi_j \psi_j \tag{41d}$$

Substituting these expressions into the weak statement in Eq.(23), the finite element model of a typical element can be expressed as the standard eigenvalue problem

$$([K] - P_0[G_1] - M_x^0[G_2] - \omega^2[M])\{\Delta\} = \{0\} \tag{42}$$

where $[K], [G_1], [G_2]$ and $[M]$ are the element stiffness matrix, the element geometric stiffness matrix due to axial force, bending moment and the element mass matrix, respectively. The explicit forms of them are given in Refs.[24-26].

In Eq.(42), $\{\Delta\}$ is the eigenvector of nodal displacements corresponding to an eigenvalue

$$\{\Delta\} = \{w\ u\ v\ \phi\}^{\mathrm{T}} \tag{43}$$

7. NUMERICAL EXAMPLES

A thin-walled composite box beam with length $l = 8$m is considered to investigate the effects of axial force, bending moment, fiber orientation and modulus ratio on the buckling loads, buckling moments, natural frequencies and corresponding vibration mode shapes as well as axial-moment-frequency interaction curves. Ten Hermitian beam elements with two nodes are used in the numerical examples. The geometry and stacking sequences of the box section are shown in Fig. 2, and the following engineering constants are used

$$E_1/E_2 = 25, G_{12}/E_2 = 0.6, \nu_{12} = 0.25 \tag{44}$$

For convenience, the following nondimensional axial force, bending moment and natural frequency are used

$$\overline{P} = \frac{P_0 l^2}{b_1^3 t E_2} \tag{45a}$$

$$\overline{M} = \frac{M_x^0 l}{b_1^3 t E_2} \tag{45b}$$

$$\overline{\omega} = \frac{\omega l^2}{b_1}\sqrt{\frac{\rho}{E_2}} \tag{45c}$$

As a first example, a simply supported composite box beam is considered. Stacking sequences of the left and right webs are angle-ply laminates $[\theta/-\theta]$ and $[-\theta/\theta]$ and the flanges laminates are assumed to be unidirectional, (Fig. 2a). All the coupling stiffnesses are zero, but E_{25} does not vanish due to unsymmetric lay-up of the webs. Effect of axial force on the critical buckling moments is shown in Table 1. The critical buckling loads ($\overline{P}_{cr}$) and the critical buckling moments ($\overline{M}_{cr}$) without axial force agree completely with those of previous papers [24,25]. In Table 2, with the presence of bending moment, the lowest three natural frequencies with and without the effect of axial force by the finite element analysis are compared to those by the orthotropy solution, which neglects the coupling effect of E_{25} from Eqs.(36a)-(36c). Tables 1 and 2 reveal that the tension force has a stiffening effect while the compressive force has a softening effect on the critical buckling moments and natural frequencies. Besides, it is clear that their change due to axial force is noticeable for all fiber angles. For unidirectional fiber direction, the lowest three natural frequencies by the finite element analysis are exactly corresponding to the first doubly coupled mode (flexural mode in y-direction and torsional mode), the first flexural mode in x-direction, the second doubly coupled mode by the orthotropy solution, respectively. As fiber angle increases, this order is a little change. The typical normal mode shapes corresponding to the lowest three natural frequencies with fiber angle $\theta = 30°$ for the case ($\overline{P} = 0.5\overline{P}_{cr}$, $\overline{M} = 0.5\overline{M}_{cr}$) are illustrated in Fig. 3. The mode shapes for other cases of ($\overline{P} = -0.5P_{cr}$, $\overline{M} = 0.5\overline{M}_{cr}$ and $\overline{P}$=0, $\overline{M} = 0.5\overline{M}_{cr}$) are similar to the corresponding ones for the case of ($\overline{P} = 0.5\overline{P}_{cr}$, $\overline{M} = 0.5\overline{M}_{cr}$) and are not plotted, although there

is a little difference between them. It can be seen in Figs. 3a and 3c that the vibration mode 1 and 3 exhibit doubly flexural-torsional coupled vibration. Due to the small coupling stiffnesses E_{25}, these coupled modes are dominated by coupling from bending moment rather than from material anisotropy. Thus, the results by the finite element analysis and orthotropy solution show slight discrepancy in ω_1 and ω_3. Since the vibration mode 2 is pure flexural x-direction mode as can be seen in Fig. 3b, the results between them are identical. It is indicated that the simple orthotropy solution is sufficiently accurate for vibration and buckling analysis of this stacking sequence (Tables 1 and 2). In order to investigate the effects of bending moment on the critical buckling loads and natural frequencies, the axial-moment and moment-frequency interaction curves with the fiber angles $\theta = 0^\circ$ and 30° are plotted in Figs. 4 and 5. It can be seen that all of the interaction curves are symmetric with respect to the y-axis. Characteristic of axial-moment and moment-frequency interaction curves is that the value of the bending moment for which the axial force or natural frequency vanishes constitutes the buckling moment. For example, for $\theta = 30^\circ$ (Fig. 5), when the beam is under an axial compressive force ($\overline{P} = 0.5\overline{P}_{cr}$), the first buckling moment occurs at $\overline{M} = 1.94$, which agrees completely with value from Table 1. As a result, the lowest branch is disappeared when $\overline{M}$ is slightly over this value. As the moment increases, two curves (ω_{xx_1}) and ($\omega_{ya_1} - M_{ya_1}$) intersect at $\overline{M} = 4.15$, thus, after this value, vibration mode 2 and 3 change each other. The third branch will also be disappeared when $\overline{M}$ is slightly over 5.14, which is corresponding to the second buckling moment. On the other hand, the natural frequencies (ω_{xx_1}) are constant for all values of bending moment. A comprehensive three dimensional axial-moment-frequency interaction diagram with the fiber angles 30° and 60° is plotted in Fig. 6. It is clear that moment-frequency interaction curves become smaller as the axial force increases, as expected. Finally, these interaction curves vanish at about $\overline{P} = 6.67$ and 13.55 for fiber angles $\theta = 30^\circ$ and 60°, respectively, which implies that at these loads, the critical buckling occurs as a degenerated case of natural vibration at zero frequency and bending moment at zero value. Fig. 6 also explains the duality among critical buckling moment, critical buckling load and fundamental natural frequency.

The next example is the same as before except that in this case, the top flange and the left web laminates are $[\theta_2]$, while the bottom flange and right web laminates are unidirectional, (Fig. 2b). Major effects of axial force and bending moment on the critical buckling moments and natural frequencies are again seen Tables 3 and 4. It is also from these tables that the coupling effects become no more negligibly small. Three dimensional fiber-moment-frequency interaction diagram with respect to the fiber angle change in the bottom flange is illustrated in Fig. 7. Three groups of curves are observed. The smallest group is for the case of axial compressive force ($\overline{P} = 0.5\overline{P}_{cr}$) and the largest one is for the case of axial tensile force ($\overline{P} = -0.5\overline{P}_{cr}$). Fig. 7 demonstrates again the fact that a tensile force stiffens the beam

while a compressive force softens the beam. The axial-moment interaction curves for various fiber angles are plotted in Fig. 8. The moment at buckling increases from zero as the axial compressive force decreases from the buckling load to the buckling moment when $P = 0$. At about $\overline{M}_{cr}$=1.26, 1.42 and 2.32 for fiber angles 90°, 60° and 30°, respectively, the critical buckling moments for pure bending occur. The lowest three moment-frequency interaction curves by the finite element analysis and orthotropy solution for the fiber angle $\theta = 60°$ with ($\overline{P} = \pm 0.5\overline{P}_{cr}$) are displayed in Figs. 9 and 10. It can be observed that the first and third natural frequencies increase, reach maximum value at $\overline{M} = 0$ and finally decrease to zero. The increase and decrease becomes more quickly when bending moments are close to buckling moments. The orthotropy and finite element solutions show discrepancy in Figs. 8-10 indicating the coupling effects become significant. It can be also explained partly by the typical normal mode shapes corresponding to the first three natural frequencies with fiber angle $\theta = 60°$ for the case ($\overline{P} = 0.5\overline{P}_{cr}$, $\overline{M} = 0.5\overline{M}_{cr}$) in Fig. 11. All three modes are triply coupled vibration, as expected (flexural mode in the x- and y-directions and torsional mode). That is, the orthotropy solution is no longer valid for unsymmetrically laminated beams, and triply flexural-torsional coupled vibration and buckling should be considered for accurate analysis even for bisymmetric thin-walled composite beams.

Finally, the effects of modulus ratio (E_1/E_2) on the first three natural frequencies of a cantilever composite beam under an axial compressive force and tensile force ($\overline{P} = \pm 0.5\overline{P}_{cr}$) and bending moment ($\overline{M} = 0.5\overline{M}_{cr}$) are investigated. The stacking sequence of the flanges and web are $[0/90]_s$, (Fig. 2c). For this lay-up, all the coupling stiffnesses vanish and thus, the three distinct vibration mode ($\omega_{ya_1}, \omega_{xx_1}$) and ($\omega_{ya_2}$) are identified. It is observed from Fig. 12 that the natural frequencies ($\omega_{ya_1}, \omega_{xx_1}$) and ($\omega_{ya_2}$) increase with increasing orthotropy (E_1/E_2) for two cases considered.

8. CONCLUDING REMARKS

Flexural-torsional coupled vibration and buckling of thin-walled composite box beams with arbitrary lay-ups under constant axial loads and equal end moments is presented. This model is based on the classical lamination theory, and accounts for all the structural coupling coming from the material anisotropy. A one-dimensional displacement-based finite element method with seven degrees of freedoms per node is developed to solve the problem. The effects of axial force, bending moment, fiber orientation on the buckling loads, buckling moments, natural frequencies and corresponding vibration mode shapes as well as axial-moment-frequency interaction curves are investigated. The tension force has a stiffening effect while the compressive force has a softening effect on the buckling moments and natural frequencies. The duality among the buckling loads, buckling moments and natural frequencies is studied. The present model is found to be appropriate and efficient in analyzing vibration and buckling problem of thin-walled

composite beams under constant axial loads and equal end moments.

Acknowledgments

The support of the research reported here by Basic Science Research Program through the National Research Foundation of Korea (NRF) funded by the Ministry of Education, Science and Technology (2009-0087819) is gratefully acknowledged. The authors also would like to thank the anonymous reviewers for their suggestions in improving the standard of the manuscript.

References

[1] V. Z. Vlasov, Thin Walled Elastic Beams, Israel Program for Scientific Transactions, Jerusalem, 1961.

[2] A. Gjelsvik, The theory of thin walled bars, Wiley, New York, 1981.

[3] F. Bleich, L. Ramsey, H. Bleich, Buckling strength of metal structures, McGraw-Hill, New York, 1952.

[4] S. Timoshenko, J. M. Gere, Theory of elastic stability, McGraw-Hill, New York, 1961.

[5] S. Timoshenko, D. H. Young, W. J. R. Weaver, Vibration problems in engineering, John Wiley & Sons, New York, 1974.

[6] A. Joshi, S. Suryanarayan, A unified solution for various boundary conditions for the coupled flexural-torsional instability of closed thin-walled beam-columns, Int J Solids Struct 20 (2) (1984) 167 – 178.

[7] A. Joshi, S. Suryanarayan, Unified analytical solution for various boundary conditions for the coupled flexural-torsional vibration of beams subjected to axial loads and end moments, J Sound Vib 129 (2) (1989) 313 – 326.

[8] R. Pavlovic, P. Kozic, P. Rajkovic, I. Pavlovic, Dynamic stability of a thin-walled beam subjected to axial loads and end moments, J Sound Vib 301 (3-5) (2007) 690 – 700.

[9] F. Mohri, C. Bouzerira, M. Potier-Ferry, Lateral buckling of thin-walled beam-column elements under combined axial and bending loads, Thin-Walled Struct 46 (3) (2008) 290 – 302.

[10] E. Magnucka-Blandzi, Critical state of a thin-walled beam under combined load, Appl Math Model 33 (7) (2009) 3093 – 3098.

[11] A. Y. T. Leung, Exact dynamic stiffness for axial-torsional buckling of structural frames, Thin-Walled Struct 46 (1) (2008) 1 – 10.

[12] A. Y. T. Leung, Dynamic axial-moment buckling of linear beam systems by power series stiffness, J Eng Mech 135 (8) (2009) 852–861.

[13] F. Mohri, L. Azrar, M. Potier-Ferry, Vibration analysis of buckled thin-walled beams with open sections, J Sound Vib 275 (1-2) (2004) 434 – 446.

[14] R. Bebiano, N. Silvestre, D. Camotim, Local and global vibration of thin-walled members subjected to compression and non-uniform bending, J Sound Vib 315 (3) (2008) 509 – 535.

[15] G. M. Voros, On coupled bending-torsional vibrations of beams with initial loads, Mech Res Commun 36 (5) (2009) 603 – 611.

[16] L. C. Bank, C. Kao, Dynamic Response of Thin-Walled Composite Material Timoshenko Beams, J Energ Resour 112 (2) (1990) 149–154.

[17] J. R. Banerjee, F. W. Williams, Exact dynamic stiffness matrix for composite Timoshenko beams with applications, J Sound Vib 194 (4) (1996) 573 – 585.

[18] J. R. Banerjee, Free vibration of axially loaded composite Timoshenko beams using the dynamic stiffness matrix method, Comput Struct 69 (2) (1998) 197 – 208.

[19] J. Li, R. Shen, H. Hua, J. Xianding, Bending-torsional coupled dynamic response of axially loaded composite Timosenko thin-walled beam with closed cross-section, Compos Struct 64 (1) (2004) 23 – 35.

[20] J. Li, J. Xianding, Coupled bending-torsional dynamic response of axially loaded slender composite thin-walled beam with closed cross-section, J Compos Mater 38 (2004) 515 – 534.

[21] M. Kaya, O. O. Ozgumus, Flexural-torsional-coupled vibration analysis of axially loaded closed-section composite Timoshenko beam by using DTM, J Sound Vib 306 (3-5) (2007) 495 – 506.

[22] N. I. Kim, D. K. Shin, Dynamic stiffness matrix for flexural-torsional, lateral buckling and free vibration analyses of mono-symmetric thin-walled composite beams, Int J Struct Stab Dy 9 (3) (2009) 411–436.

[23] S. P. Machado, V. H. Cortinez, Free vibration of thin-walled composite beams with static initial stresses and deformations, Eng Struct 29 (3) (2007) 372 – 382.

[24] J. Lee, S. E. Kim, K. Hong, Lateral buckling of I-section composite beams, Eng Struct 24 (7) (2002) 955 – 964.

[25] T. P. Vo, J. Lee, Flexural-torsional buckling of thin-walled composite box beams, Thin-Walled Struct 45 (9) (2007) 790 – 798.

[26] T. P. Vo, J. Lee, Free vibration of axially loaded thin-walled composite box beams, Compos Struct 90 (2) (2009) 233 – 241.

[27] R. M. Jones, Mechanics of Composite Materials, Taylor & Francis, 1999.

CAPTIONS OF TABLES

Table 1: Effect of axial force on the critical buckling moments ($\overline{M}_{cr}$) of a simply supported composite box beam with respect to the fiber angle change in the webs.

Table 2: Effect of axial force and bending moment on the first three natural frequencies of a simply supported composite box beam with respect to the fiber angle change in the webs.

Table 3: Effect of axial force on the critical buckling moments ($\overline{M}_{cr}$) of a simply supported composite box beam with respect to the fiber angle change in the left web and top flange.

Table 4: Effect of axial force and bending moment on the first three natural frequencies of a simply supported composite box beam with respect to the fiber angle change in the left web and top flange.

CAPTIONS OF FIGURES

Figure 1: Definition of coordinates in thin-walled closed sections.

Figure 2: Geometry and stacking sequences of thin-walled composite box beam.

Figure 3: The first three normal mode shapes of the flexural and torsional components with the fiber angle 30° in the webs of a simply supported composite box beam under an axial compressive force and bending moment ($\overline{P} = 0.5\overline{P}_{cr}$, $\overline{M} = 0.5\overline{M}_{cr}$).

Figure 4: Effect of axial force on the critical buckling moments with the fiber angles 0° and 30° in the webs of a simply supported composite box beam.

Figure 5: Effect bending moment on the first three natural frequencies with the fiber angles 0° and 30° in the webs of a simply supported composite box beam under an axial compressive force ($\overline{P} = 0.5\overline{P}_{cr}$).

Figure 6: Three dimensional interaction diagram between the fundamental natural frequency and bending moment with respect to the axial force change with the fiber angles 30° and 60° in the webs of a simply supported composite box beam.

Figure 7: Effect of axial force on three dimensional interaction diagram between the fundamental natural frequency and bending moment with respect to the fiber angle change in the left web and top flange of a simply supported composite box beam.

Figure 8: Effect of axial force on the critical buckling moments with the fiber angles 30° and 60° in the left web and top flange of a simply supported composite beam.

Figure 9: Effect of bending moment on the first three natural frequencies with the fiber angle 60° in the left web and top flange of a simply supported composite box beam under an axial compressive force ($\overline{P} = 0.5\overline{P}_{cr}$).

Figure 10: Effect of bending moment on the first three natural frequencies with the fiber angle 60° in the left web and top flange of a simply supported composite box beam under an axial tensile force ($\overline{P} = -0.5\overline{P}_{cr}$).

Figure 11: The first three normal mode shapes of the flexural and torsional components with the fiber angle 60° in the left web and top flange of a simply supported composite box beam under an axial compressive force and bending moment ($\overline{P} = 0.5\overline{P}_{cr}$, $\overline{M} = 0.5\overline{M}_{cr}$).

Figure 12: Variation of the first three natural frequencies with respect to modulus ratio change of a cantilever composite beam under axial force and bending moment ($\overline{P} = -0.5\overline{P}_{cr}$, $\overline{M} = 0.5\overline{M}_{cr}$) and ($\overline{P} = 0.5\overline{P}_{cr}$, $\overline{M} = 0.5\overline{M}_{cr}$).

TABLE 1 Effect of axial force on the critical buckling moments ($\overline{M}_{cr}$) of a simply supported composite box beam with respect to the fiber angle change in the webs.

Fiber	Buckling	$\overline{P} = 0.5\overline{P}_{cr}$ (compression)		$\overline{P}$=0 (no axial force)		$\overline{P} = -0.5\overline{P}_{cr}$ (tension)	
angle	loads ($\overline{P}_{cr}$)	Present	Orthotropy	Present	Orthotropy	Present	Orthotropy
0	36.009	1.891	1.891	2.688	2.688	3.309	3.309
15	29.245	2.629	2.632	3.725	3.729	4.571	4.575
30	13.549	1.945	1.946	2.753	2.755	3.374	3.376
45	7.858	1.217	1.217	1.722	1.722	2.111	2.111
60	6.670	0.941	0.941	1.332	1.332	1.633	1.633
75	6.419	0.830	0.830	1.175	1.175	1.441	1.441
90	6.375	0.798	0.798	1.131	1.131	1.386	1.386

TABLE 2 Effect of axial force and bending moment on the first three natural frequencies of a simply supported composite box beam with respect to the fiber angle change in the webs.

Fiber	Axial force	Present			Orthotropy			
angle	& moment	ω_1	ω_2	ω_3	ω_{ya_1}	ω_{yb_1}	ω_{xx_1}	ω_{ya_2}
0		6.656	16.704	39.937	6.656	74.746	16.704	39.937
30	$\overline{P} = 0.5\overline{P}_{cr}$	4.088	14.750	24.511	4.090	125.266	14.750	24.531
60	$\overline{M} = 0.5\overline{M}_{cr}$	2.868	14.097	17.209	2.868	86.303	14.097	17.209
90		2.804	14.068	16.823	2.804	74.929	14.068	16.823
0		9.401	18.392	42.041	9.401	75.242	18.392	42.041
30	$\overline{P} = 0$	5.780	15.487	25.835	5.782	125.396	15.487	25.854
60	$\overline{M} = 0.5\overline{M}_{cr}$	4.055	14.481	18.137	4.055	86.407	14.481	18.137
90		3.964	14.436	17.730	3.964	75.044	14.436	17.730
0		11.499	19.937	44.034	11.499	75.736	19.937	44.034
30	$\overline{P} = -0.5\overline{P}_{cr}$	7.078	16.191	27.093	7.080	125.526	16.191	27.111
60	$\overline{M} = 0.5\overline{M}_{cr}$	4.966	14.855	19.019	4.966	86.511	14.855	19.019
90		4.854	14.795	18.591	4.854	75.159	14.795	18.591

TABLE 3 Effect of axial force on the critical buckling moments ($\overline{M}_{cr}$) of a simply supported composite box beam with respect to the fiber angle change in the left web and top flange.

Fiber	Buckling	$\overline{P} = 0.5\overline{P}_{cr}$ (compression)		$\overline{P}$=0 (no axial force)		$\overline{P} = -0.5\overline{P}_{cr}$ (tension)	
angle	loads ($\overline{P}_{cr}$)	Present	Orthotropy	Present	Orthotropy	Present	Orthotropy
0	36.009	1.891	1.891	2.688	2.688	3.309	3.309
15	30.210	1.922	2.599	2.741	3.595	3.366	4.376
30	17.015	1.625	2.180	2.322	2.960	2.834	3.576
45	9.899	1.232	1.502	1.748	1.977	2.133	2.360
60	7.918	1.008	1.232	1.427	1.584	1.743	1.871
75	7.454	0.909	1.121	1.285	1.431	1.571	1.686
90	7.370	0.881	1.089	1.246	1.389	1.523	1.635

TABLE 4 Effect of axial force and bending moment on the first three natural frequencies of a simply supported composite box beam with respect to the fiber angle change in the left web and top flange.

Fiber	Axial force	Present			Orthotropy			
angle	& moment	ω_1	ω_2	ω_3	ω_{ya_1}	ω_{yb_1}	ω_{xx_1}	ω_{ya_2}
0		6.656	16.704	39.937	6.656	74.746	16.704	39.937
30	$\overline{P} = 0.5\overline{P}_{cr}$	4.656	13.113	23.652	5.355	114.467	13.160	29.157
60	$\overline{M} = 0.5\overline{M}_{cr}$	3.135	11.918	18.624	4.083	81.416	11.635	21.522
90		3.020	11.867	18.095	4.038	72.595	11.567	21.085
0		9.401	18.392	42.041	9.401	75.242	18.392	42.041
30	$\overline{P} = 0$	6.555	14.139	25.438	7.200	114.610	14.183	30.701
60	$\overline{M} = 0.5\overline{M}_{cr}$	4.429	12.458	19.650	5.131	81.512	12.182	22.397
90		4.269	12.375	19.074	5.023	72.695	12.080	21.911
0		11.499	19.937	44.034	11.499	75.736	19.937	44.034
30	$\overline{P} = -0.5\overline{P}_{cr}$	8.038	15.093	27.118	8.671	114.753	15.138	32.183
60	$\overline{M} = 0.5\overline{M}_{cr}$	5.427	12.973	20.629	6.003	81.608	12.706	23.244
90		5.230	12.859	20.007	5.848	72.795	12.572	22.710

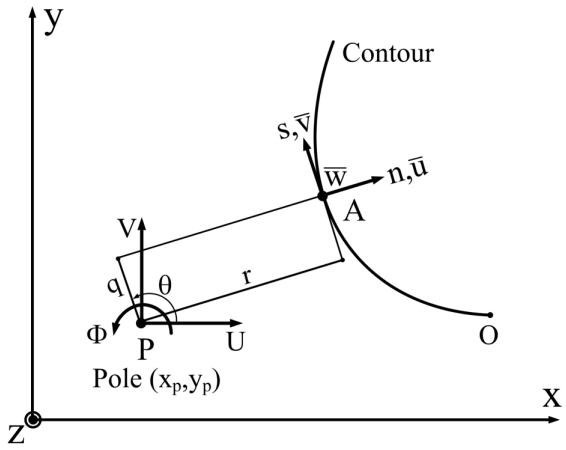

FIG. 1 Definition of coordinates in thin-walled closed sections

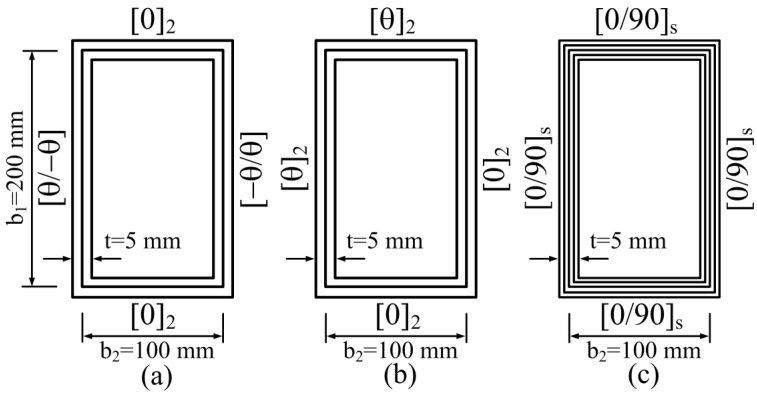

FIG. 2 Geometry and stacking sequences of thin-walled composite box beam.

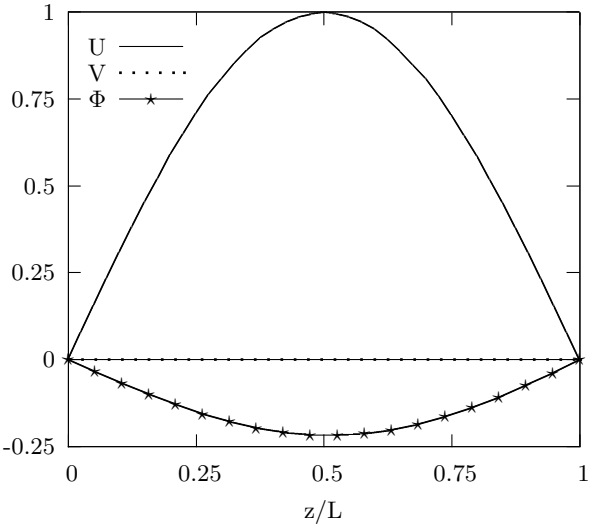

(a) Mode 1

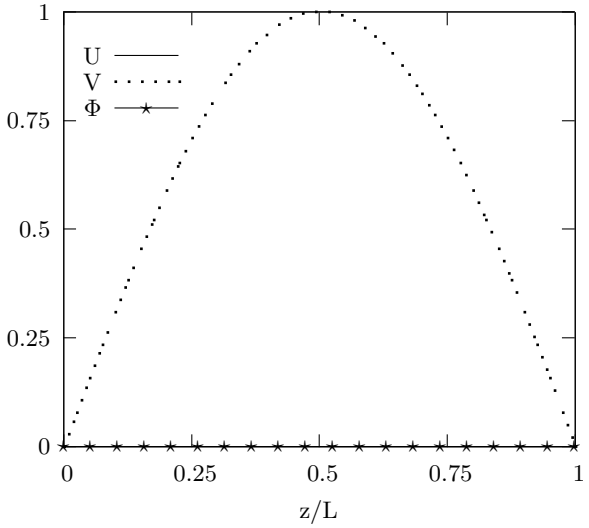

(b) Mode 2

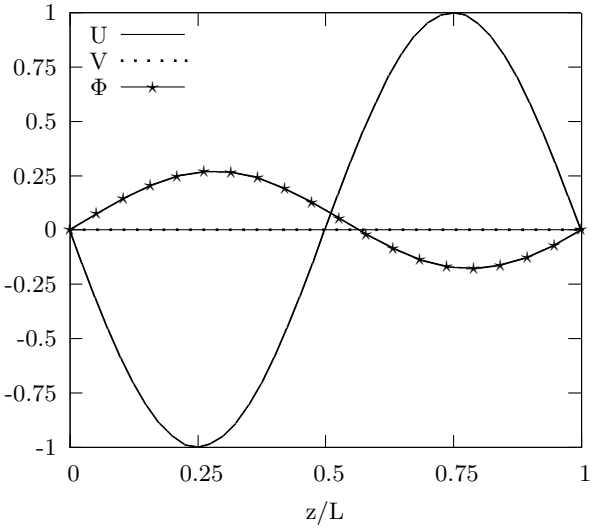

(c) Mode 3

FIG. 3 The first three normal mode shapes of the flexural and torsional components with the fiber angle 30° in the webs of a simply supported composite box beam under an axial compressive force and bending moment ($\overline{P} = 0.5\overline{P}_{cr}$, $\overline{M} = 0.5\overline{M}_{cr}$).

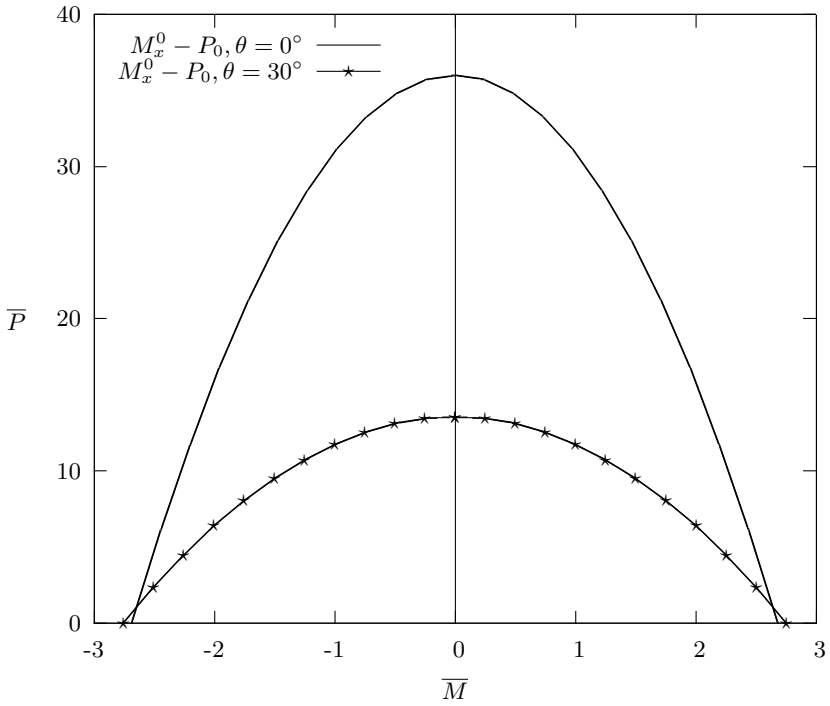

FIG. 4 Effect of axial force on the critical buckling moments with the fiber angles 0° and 30° in the webs of a simply supported composite box beam.

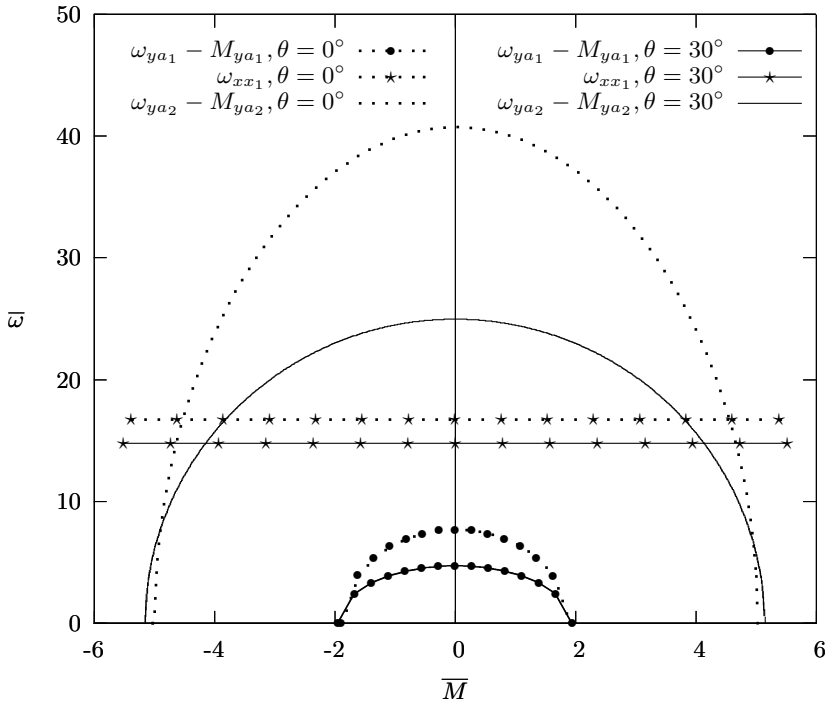

FIG. 5 Effect of bending moment on the first three natural frequencies with the fiber angles 0° and 30° in the webs of a simply supported composite box beam under an axial compressive force ($\overline{P} = 0.5\overline{P}_{cr}$).

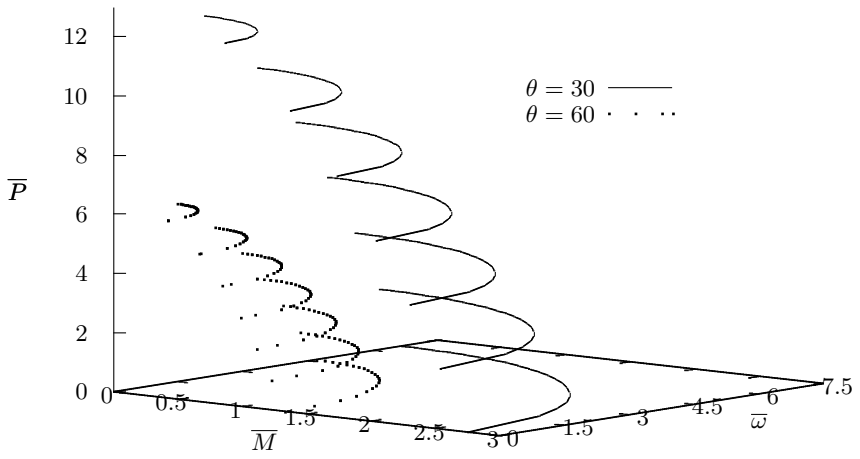

FIG. 6 Three dimensional interaction diagram between the fundamental natural frequency and bending moment with respect to the axial force change with the fiber angles 30° and 60° in the webs of a simply supported composite box beam.

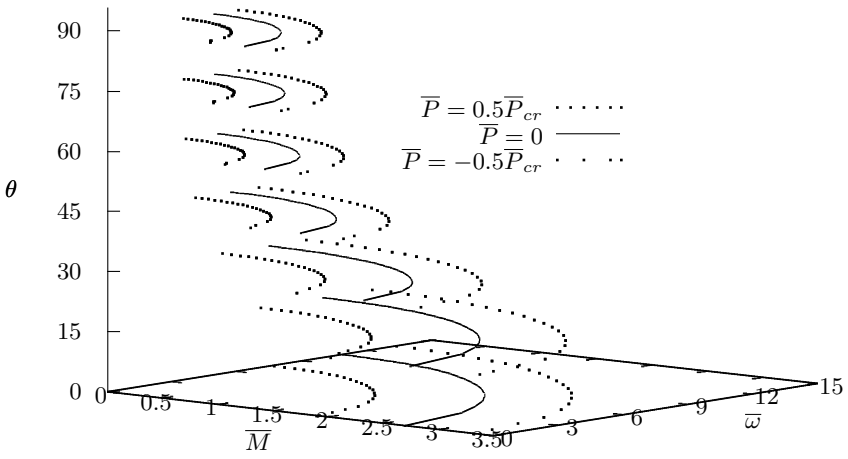

FIG. 7 Effect of axial force on three dimensional interaction diagram between the fundamental natural frequency and bending moment with respect to the fiber angle change in the left web and top flange of a simply supported composite box beam.

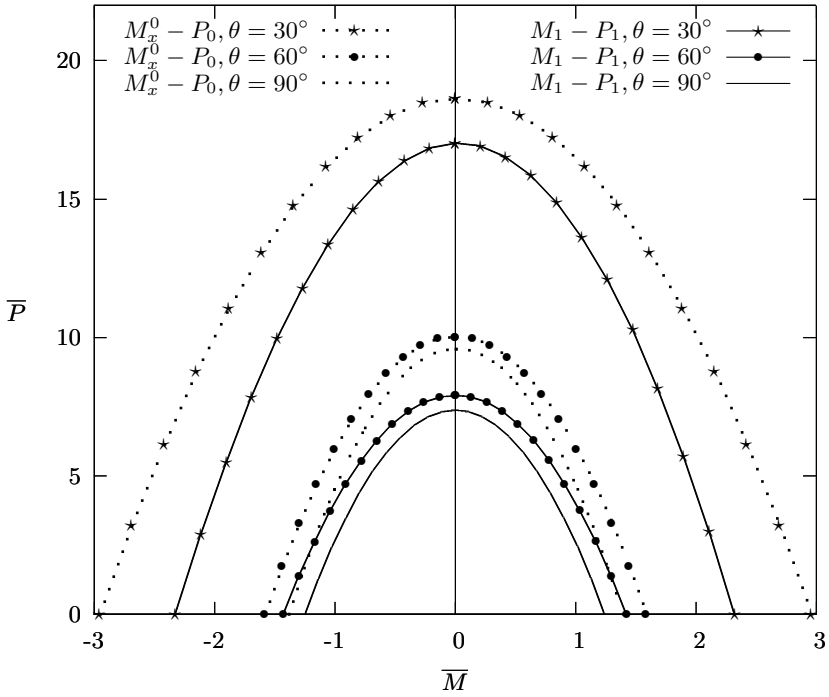

FIG. 8 Effect of axial force on the critical buckling moments with the fiber angles $30°, 60°$ and $90°$ in the left web and top flange of a simply supported composite box beam.

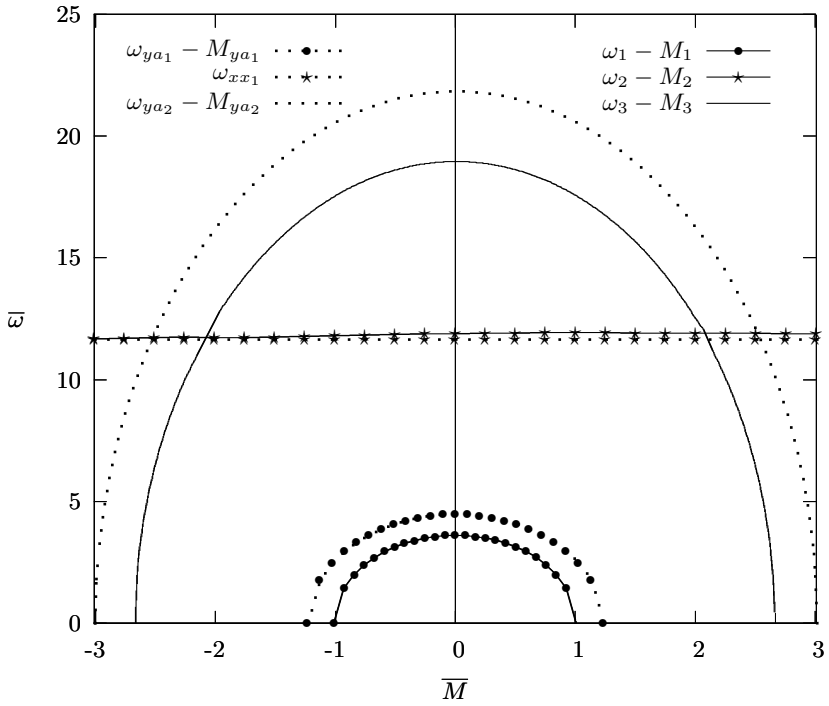

FIG. 9 Effect of bending moment on the first three natural frequencies with the fiber angle 60° in the left web and top flange of a simply supported composite box beam under an axial compressive force ($\overline{P} = 0.5\overline{P}_{cr}$).

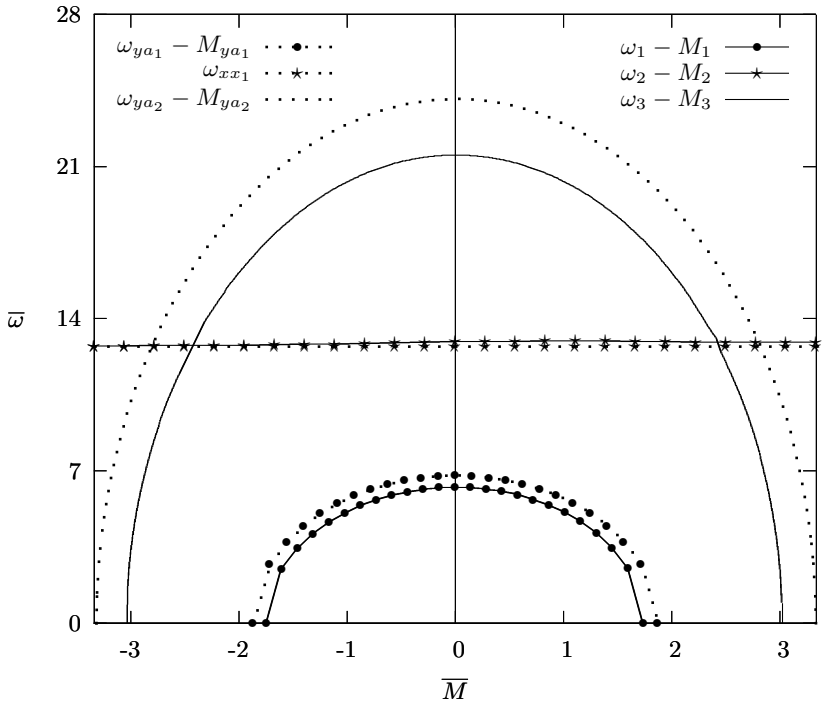

FIG. 10 Effect of bending moment on the first three natural frequencies with the fiber angle 60° in the left web and top flange of a simply supported composite box beam under an axial tensile force ($\overline{P} = -0.5\overline{P}_{cr}$).

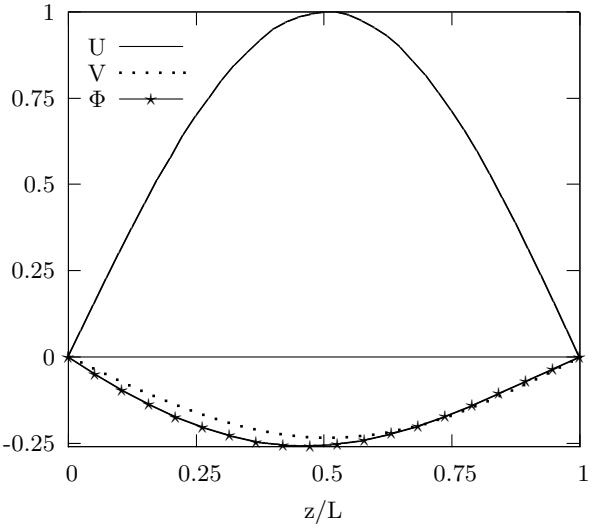

(a) Mode 1

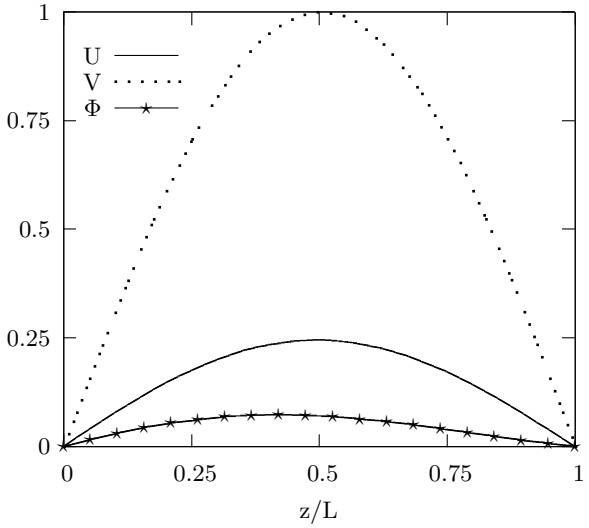

(b) Mode 2

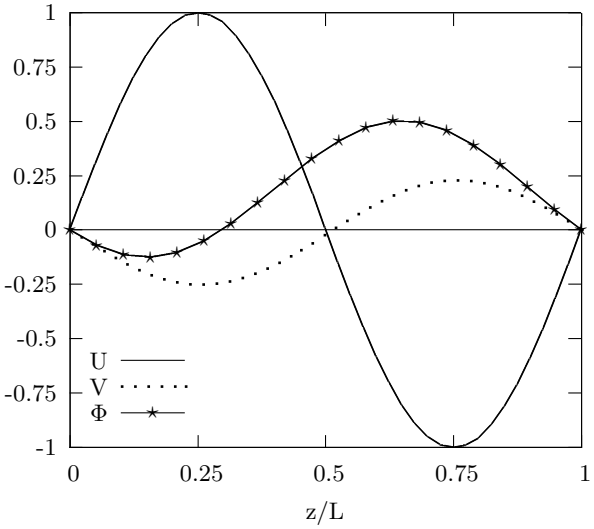

(c) Mode 3

FIG. 11 The first three normal mode shapes of the flexural and torsional components with the fiber angle 60° in the left web and top flange of a simply supported composite box beam under an axial compressive force and bending moment ($\overline{P} = 0.5\overline{P}_{cr}$, $\overline{M} = 0.5\overline{M}_{cr}$).

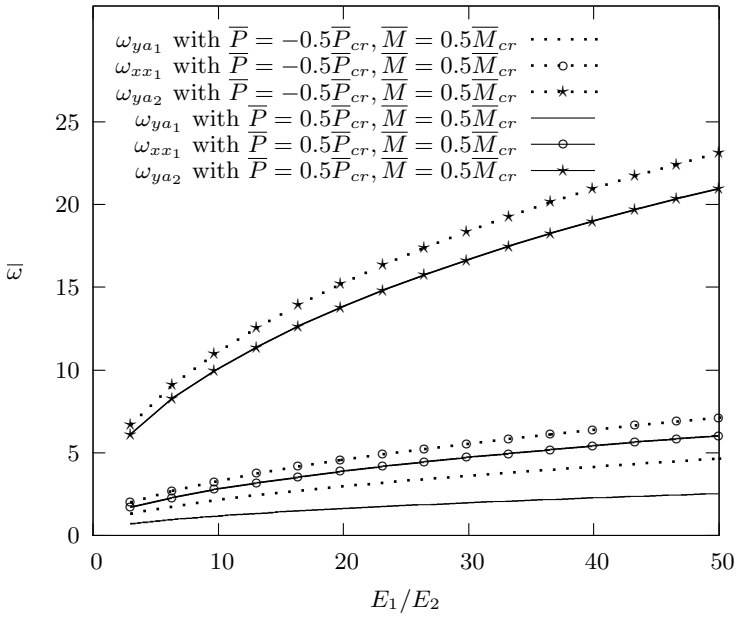

FIG. 12 Variation of the first three natural frequencies with respect to modulus ratio change of a cantilever composite beam under axial force and bending moment ($\overline{P} = -0.5\overline{P}_{cr}$, $\overline{M} = 0.5\overline{M}_{cr}$) and ($\overline{P} = 0.5\overline{P}_{cr}$, $\overline{M} = 0.5\overline{M}_{cr}$).